Time-dependent compressive deformation of the ageing spine: relevance to spinal stenosis.

P. Pollintine*, M.S.L.M van Tunen+, J. Luo, M. Brown, P. Dolan, M.A. Adams

Department of Anatomy, University of Bristol, Bristol, UK

*Department of Mechanical Engineering, University of Bath, Bath, U.K.

+ Amsterdam, Netherlands

Revised version, re-submitted to Spine, 14th April 2009

Corresponding author:
Dr Michael A. Adams,
Reader in Spine Biomechanics,
Department of Anatomy,
University of Bristol,
Southwell Street,
Bristol BS2 8EJ, U.K.

M.A.Adams@bris.ac.uk

Tel: +44 (0) 117 928 8363

Fax: +44 (0) 117 925 4794

KEY WORDS: vertebra; intervertebral disc; deformation; creep; age; strain.

Acknowledgements: Research funded in the U.K. by BBSRC and Action Medical Research.

Abstract

Study Design Mechanical testing of cadaveric spines.

Summary of Background Data Intervertebral discs and vertebrae deform under load, narrowing the intervertebral foramen and increasing the risk of nerve root entrapment. Little is known about compressive deformations when elderly spines are subjected to sustained physiological loading.

Objective To test the hypothesis that, in the ageing spine, vertebrae deform more than discs, and contribute to time-dependent creep.

Methods 117 thoracolumbar motion segments, aged 19-96 (mean 69) yr, were subjected to 1kN compressive loading for 0.5, 1 or 2hr. Deformations during the first 7s were designated "elastic" and subsequent deformations as "creep". A three-parameter model was fitted to experimental data in order to characterise their viscous modulus E1, elastic modulus E2 (initial stiffness), and viscosity η (resistance to fluid flow). Intradiscal pressure (IDP) was measured using a miniature needle-mounted transducer. In 17 specimens loaded for 0.5hr, an optical MacReflex system measured compressive deformations separately in the disc and each vertebral body.

Results On average, the disc contributed 28% of the spine's elastic deformation, 51% of the creep deformation, and 38% of total deformation. Elastic, creep, and total deformations of 84 motion segments in 2hr tests averaged 0.87mm, 1.37mm and 2.24mm respectively. Measured deformations were predicted accurately by the model (average r^2=0.97) but E1, E2 and η depended on the duration of loading. E2 and η decreased with advancing age and disc degeneration, in proportion to falling IDP ($p<0.001$). Total compressive deformation increased with age, but rarely exceeded 3mm.

Conclusions When the ageing spine is compressed, vertebral bodies show greater elastic deformations than intervertebral discs, and creep by a similar amount. Responses to axial compression depends largely on IDP, but deformations appear to be limited by impaction of adjacent neural arches. Total compressive deformations are sufficient to cause foraminal stenosis in some individuals.

Précis

When ageing cadaveric spines were subjected to sustained physiological loading, elastic (immediate) deformations were greater in the vertebral bodies than in the intervertebral discs, and creep deformations were similar in both structures. Total compressive deformations were sufficient to cause foraminal stenosis in some individuals.

Key Points

1. Excessive compressive deformations of the spine under load could lead to nerve root entrapment in the intervertebral foramen, and to abnormally high loading of the apophyseal joints.
2. Experiments on 117 cadaveric thoracolumbar motion segments showed that ageing vertebral bodies deform more than their adjacent discs in response to sustained compressive loading. Both structures showed substantial "creep".
3. Responses of the disc/vertebral body unit to axial compression depend largely on intradiscal pressure. Compressive deformations increase with age as disc pressure falls, but deformations appear to be limited by impaction of adjacent neural arches.
4. Total compressive deformations are sufficient to cause foraminal stenosis in some individuals.

Introduction

Vertebrae and intervertebral discs deform under load, sometimes with important clinical consequences. Most obviously, they reduce the volume of the intervertebral foramen and increase the risk of nerve root entrapment syndromes.[1-3] Compressive deformations also bring adjacent neural arches closer together, and can cause them to play a major load-bearing role,[4] with adverse consequences for the apophyseal joints.[5, 6] Both neurogenic claudication and facet joint pain are sensitive to physical activity and posture, suggesting that they can be caused by inadequate separation of vertebrae. However, little is known about the magnitude of compressive deformations when the ageing spine is subjected to substantial compressive loading.

Intervertebral discs are relatively soft in order to spread load evenly on the adjacent vertebral bodies, and to allow substantial intervertebral movements. Vertebrae, in contrast, must be stiff to maintain the geometry of their articulations under load, and to move quickly when acted on by muscles. However, the traditional concept of rigid vertebrae separated by deformable discs is an over-simplification, especially in the elderly spine. Age-related reductions in bone mineral density (BMD) lead to weakened vertebrae which deform markedly under load[7-9] and which can "creep" gradually under static loading. [10, 11] Intervertebral discs are softer than vertebrae, but their relatively small height means they deform little. It would be expected, therefore, that discs and vertebrae would both contribute substantially towards the deformation of an elderly spine subjected to vigorous and sustained compressive loading.

There have been many previous attempts to measure disc and vertebral deformations in cadaveric spines, but most of the experiments suffer from one or more technical limitations. Usually, the maximum applied force was chosen to simulate upper body weight (approximately 400N), and so disregarded the muscle forces that are now known to raise spinal compression in-vivo to 800-1200N during upright postures[12] and to 3-5kN during manual work.[13] Another limitation is that most experiments measured the overall deformation of a spine motion segment and attributed it all to the disc. Finally, it has generally been assumed that only the discs exhibit "creep" (time-dependent deformations under constant load) even though bone creep has been demonstrated in small tissue samples[14, 15] and more recently, in whole vertebrae.[16] A few attempts have been made to overcome these difficulties, for example by using radiographs to measure vertebral deformations[8] or optical and MRI techniques to measure deformations of intervertebral discs.[17-19] However measurements comparing disc and vertebral deformations in elderly spines are lacking, and deformations of both structures have not been tracked over time.

The present study aims to characterise time-dependent compressive deformations of discs and vertebrae in the ageing thoracolumbar spine, and to assess their clinical significance. Mechanical

experiments on many motion segments were analysed in order to quantify the competing influences of age, spinal level and disc degeneration. Loading regimes were substantial and chronic in order to simulate physiological loading in-vivo, and an optical strain measuring device was used to differentiate between disc and vertebral deformations in some of the specimens.

Materials and Methods

Cadaveric material

Sixty-one thoracolumbar spines were removed from cadavers donated to medical research. None of the donors had experienced prolonged bed rest or spinal injury before death. Spines were dissected into 117 "motion segments" consisting of two adjacent vertebrae and the intervening disc and ligaments. All levels were included between T7-8 and L4-5, with the following distribution: T7-8 (3), T8-9 (4), T9-10 (5), T10-11 (10), T11-12 (11), T12-L1 (11), L1-2 (18), L2-3 (20), L3-4 (14), L4-5 (21). Mean age of motion segments was 69 yr (range 19-96, STD 17 yr) They were wrapped in clingfilm, double bagged, and stored at -20^{o}C for up to three months before testing. Specimens were used in a variety of experiments over several years, but the present study considers only the initial creep test that was performed on all of them as part of routine pre-conditioning. For this reason, some experimental details varied between groups of specimens, including the duration of loading.

Radiography and specimen preparation

Motion segments were defrosted overnight at 3°C, and then radiographed in the frontal and sagittal plane. Films were scanned and analysed using 'ImageJ' software to enable disc and vertebral dimensions to be measured. Disc height was determined separately for the anterior and posterior annulus, and for the nucleus, and an average of the three heights (h) obtained. Cross sectional area (A) of the disc was estimated from the frontal (α) and sagittal plane (β) diameters of the superior vertebral endplate, using the equation for the area of an ellipse: $A = \alpha\pi\beta/4$. Grade of disc degeneration was assessed after testing, using the first four points on a morphological and functional scale published previously.[20, 21]

Each motion segment was secured in two metal cups containing dental plaster (**Figure 1)**. Screws in the neural arch enhanced fixation between bone and plaster, but care was taken that the outer surfaces of the vertebral bodies merely rested on the plaster rather than being immersed in it. Cling film was wrapped around exposed surfaces of the specimen to minimise water loss.

Compressive creep-loading experiments

Motion segments were tested at room temperature on a computer-controlled hydraulic materials

testing machine (Dartec/Zwick Roell Ltd., Leominster, UK). Two low-friction rollers **(**Figure 1) applied a pure compressive force in the direction perpendicular to the mid-plane of the disc, while minimizing any anterior-posterior shear. This apparatus has been used previously to apply compressive loading across a motion segment.[22] Initially, a compressive force of 300N was applied for 15 minutes to expel some water from the disc and to guard against the possibility of post-mortem super-hydration.[23] This was followed immediately by the main creep test, as follows. A compressive force (mean 1.15 kN, STD 0.25 kN) was applied in linear ramp fashion over 5s and then held constant for up to two hours, with the Dartec operating in "load-control". This force is sufficient to simulate gravitational and muscle forces acting on the upright spine during upright activities in-vivo.[12] It was varied slightly to take some account of specimen age and size. Applied stress (load divided by average endplate area) averaged 0.85 MPa (STD 0.28 MPa). Vertical (compressive) deformation of the whole specimen and cups was measured at 1 Hz by a linear variable differential transformer (LVDT) attached to the ram of the testing machine. Compressive force was also monitored at 1 Hz. 'Elastic deformation' was defined as all deformation recorded during load application (5s) and in the first 2s after load application. 'Creep deformation' was measured as the continuing deformation during the following period of static loading.

Intradiscal pressure measurements

Before the compression tests, a miniature pressure transducer (Gaeltec, Dunvegan, Scotland), side-mounted in a 1.3-mm diameter needle, was pulled through the intervertebral disc while the specimen was loaded to 1kN for 20 s.[24] Transducer output indicates fluid pressure within the nucleus[24], and within the anulus it indicates the average compressive stress acting perpendicular to its membrane.[25] These measurements were performed on 60 motion segments in order to show how intradiscal pressure (IDP) within the nucleus influences motion segment deformations under load.[26]

Deformation of disc and vertebral bodies measured using MacReflex

In 17 motion segments, vertical deformations of the intervertebral disc and each vertebral body were measured separately using an optical 2D MacReflex system (Qualisys Ltd., Goteborg, Sweden) operating at 1 Hz. This located the geometric centre of small reflective markers attached to pins inserted into the vertebrae (Figure 1) and yielded values of the anterior, middle and posterior height of each disc and each vertebral body in the sagittal plane, with a resolution of <10 μm.[9, 22] Raw data from the MacReflex was subjected to 30-point smoothing in order to reduce random errors. MacReflex measurements enabled overall vertical deformations measured by the Dartec to be apportioned between the disc, vertebral bodies, and apparatus. Vertebral strains were multiplied by vertebral body height (measured from radiographs) to calculate vertebral body deformations (in mm). This assumes that strain does not vary with vertical location in the body. Because all marker

pins had to be anchored firmly in bone, two thin strips of bone adjacent to the discs were included in the "disc height" as measured by the MacReflex. The combined height of these two strips averaged 4.8 mm. For each specimen, this combined height of bone was multiplied by the average bone strain measured for the two vertebrae in order to calculate how much bone deformation was included in the apparent disc deformation. Once this spurious deformation had been removed, the "corrected" disc deformation was divided by disc height (from radiographs) in order to calculate true disc strain.

"Three-Parameter" model of motion segment compressive deformation

A 3-parameter viscoelastic model comprising two springs and a dashpot[27] was used to model the experimental data (**Figure 2**). The purpose of modelling was to extract three parameters which characterise the time-dependent compressive deformation of each motion segment[27] or disc[28], and which enable comparisons to be made between specimens, and with previous work. A program written in Matlab (Matlab v7.0.4, Mathworks Inc., Natick, MA.) used the following function to fit the motion segment displacement data (y):

$$y(mm) = A_2 + (A_1 - A_2)\exp(-\lambda t)) \qquad \text{(Eq. 1)}$$

where A_2 is the instantaneous elastic displacement, A_1 is the total displacement after creep, and λ is a measure of creep rate. These values were then used to calculate the viscous modulus (E1), the elastic modulus (E2), and the viscosity coefficient (η) as follows:

$$E_1 = \frac{\sigma}{\varepsilon} = \frac{F/A}{(A_1 - A_2)/h} \qquad \text{(Eq. 2)}$$

$$E_2 = \frac{\sigma}{\varepsilon} = \frac{F/A}{A_2/h} \qquad \text{(Eq. 3)}$$

$$\eta = \frac{E_1}{\lambda} \qquad \text{(Eq. 4)}$$

where σ is the applied compressive stress (force per unit area), ε is strain (disc deformation divided by original height), and A and h represent disc area and height, as defined above. An iterative routine calculated which values of A1, A2 and λ in Equation 1 best fitted the experimental deformations. Best fit was expressed by the coefficient of determination (r^2). E1, E2 and η were then calculated from Equations 2-4.

Data from tests which lasted 2 hr and 1 hr were often analysed at shorter time periods also (for example, the first half of the data from a 1 hr test might be analysed at 0.5 hr). However, technical problems including data loss prevented this from being done in every case.

Statistical analyses

Linear regression was used to determine how variable factors (such as age and IDP) influenced E1, E2 and η. Stepwise linear regression was used to compare their relative influences. Influences of gender, spinal region, and category of disc degeneration were examined by ANOVA using 'SPSS'.

Results

The MacReflex system was able to distinguish between height lost by the disc and vertebrae of each motion segment. **Figure 3** shows typical deformations averaged across the anterior, middle and posterior regions. Initial elastic height loss is followed by gradual creep during the remainder of the 0.5 hr experiment. Height loss in Figure 3 is expressed as "microstrain" where 10,000 microstrain represents 1% loss of original height (of the disc or vertebral body). It is evident from the Figure that elastic strains in the disc are greater than those in the adjacent vertebral bodies, and that creep strains are much greater in the disc. Average elastic and creep strains in the 17 discs were 2.3% and 2.5% respectively, and in the 34 vertebral bodies were 0.85% and 0.44%.

Actual deformations (in mm) of discs and vertebrae are equal to measured strain multiplied by the initial height of each structure. Because a typical vertebral body is 3-4 times taller than a disc, deformations tend to be greater in the vertebrae, as shown in **Table 1.** This summarises disc and vertebral body height loss for the posterior, middle and anterior regions. Vertebral bodies lost more height anteriorly than posteriorly, whereas discs lost more height posteriorly. **Figure 4** compares height loss for each structure, averaged across the posterior, middle and anterior regions. Calculations based on this data show that, on average, the disc contributed 28% of the elastic compressive deformation of the basic repeating unit of the spine (disc + 1 vertebral body), 51% of its creep, and 38% of total (elastic+creep) deformation during the 0.5 hr tests. (The disc's contribution to motion segment deformation was rather less, because motion segments contain two vertebrae to only one disc.) If height lost by the vertebrae and disc of a motion segment is subtracted from the specimen height loss measured by the LVDT of the Dartec, there remains an average 14.7% of the deformation to account for. This is attributable to compression of the apparatus, cement and bone-cement interface.

The great variability of results evident in Table 1 and Figure 4 is largely due to random errors generated when the MacReflex system attempts to resolve very small movements of reflective markers. Average values are robust, but individual results vary greatly, and regression analysis on these 17 specimens showed no consistent trends with age or spinal level. This problem was avoided in most experiments by measuring overall motion segment height loss from the LVDT of the Dartec. These measurements were then used by the three-parameter model to calculate E1, E2 and

η for each specimen. Goodness of fit was usually excellent, but declined somewhat in the shorter tests: on average, "r^2" in the 2 hr, 1 hr and 0.5 hr tests was 0.97 (STD 0.03), 0.91 (STD 0.03) and 0.83 (STD 0.08) respectively. Discrepancies between experiment and theory were greatest at the start of the creep period. In 8/60 of the 0.5 hr tests, and 2/102 of the 1 hr tests, E2 was overestimated by more than 500%, and η was close to zero, so these 10 results were discarded as outliers. It appears that the curve-fitting algorithm was not always able to locate the transition from elastic to creep deformation accurately when the creep period was short *and* the specimen showed rapid initial creep. Calculated values of E1, E2 and η depended on test duration (**Figure 5**) and so do not represent invariant characteristics of the specimens tested. Systematic variations in Figure 5 facilitate comparisons with previous experiments performed over varying time periods.

Average values of E1, E2 and η are presented in **Table 2** for various groups of motion segments subjected to the 2 hr test. (These tests were the longest and least prone to curve-fitting problems.) E1 varied little between groups. Female motion segments had higher elastic modulus E2 and higher viscosity η ($p<0.01$). Thoracic motion segments also had higher E2 and η than did lumbar ($p<0.01$). Systematic influences on E1, E2 and η were analysed using linear regression (**Table 3)**. E1 increased with applied stress. Elastic modulus E2 decreased in discs that were degenerated or had a low IDP, and decreased in discs aged over 50 yrs (**Figure 6**). E2 also decreased at lower spinal levels, as disc area increased, and increased with increasing applied stress. Viscosity η varied in a similar manner to E2, decreasing markedly with age and increasing with IDP (**Figure 7)**. Creep rate λ, which is inversely related to viscosity as shown in Equation 4, averaged 0.51×10^{-3} /s (STD 0.21). Creep rate increased with age ($P<0.001$), especially after age 50 yrs, and decreased as IDP increased ($P=0.02$). Similar trends were seen in data from the 0.5 and 1 hr tests.

Analysing the 2 hr tests using stepwise multiple linear regression (with age, disc degeneration, IDP, disc area, disc height and spinal level as the independent variables) showed that E1 depended on spinal level ($p<0.001$) and disc area ($p=0.012$). E2 depended on disc area ($p<0.001$) and disc height ($p=0.02$). Viscosity η was influenced only by IDP ($p<0.001$). When the relative influences of age, disc degeneration and IDP were compared by forcing the three variables into the analysis, none of them predicted E1, and IDP was the only significant predictor of E2 ($p<0.001$, $r^2=0.37$) and η ($p<0.001$, $r^2=0.36$).

Elastic and creep deformations of motion segments were quantified from the model output as A2 and (A1-A2) respectively. **Table 4** summarises results for 0.5 hr, 1 hr and 2 hr tests. Creep increased from 0.54 mm in the 0.5 hr tests to 1.37 mm in the 2 hr tests. Elastic deformations also increased slightly, even though the applied stress and ages were similar between groups. Total deformation averaged 1.16 mm and 2.24 mm in the 0.5 hr and 2 hr tests respectively. Elastic, creep

and total deformations showed mostly non-significant increases with age in the 0.5, 1, and 2 hr tests, but total deformation rarely exceeded 3 mm. In the 1 hr tests, total deformation increased significantly (p=0.023) for specimens aged >50 yr (**Figure 8)**, but tended to *decrease* between the ages of 19 and 50 yr (p = 0.07), albeit on only 12 specimens.

Discussion

Summary of findings When elderly cadaveric motion segments were subjected to sustained physiological compressive loading, elastic deformations were greater in the vertebral bodies than in the disc, whereas creep deformations were similar in both structures. Measured deformations were predicted accurately by the three-parameter model, but E1, E2 and η depended on the duration of loading. Motion segment elastic stiffness (E2) and viscosity (η) decreased with advancing age and disc degeneration, and were directly proportional to intradiscal pressure. Total measured compressive deformation generally increased with age, but rarely exceeded 3 mm.

Strengths and weaknesses of the study. This was a large study on human spines. Sufficient compression was applied to simulate muscle tension as well as gravitational loading, and the 2-D MacReflex system was sensitive enough to differentiate between deformations of the disc, vertebrae and apparatus. Weaknesses of the study include MacReflex measurements being in the sagittal plane only, and a simple viscoelastic model whose parameters (E1, E2 and η) varied with testing conditions and so did not represent invariant materials properties. Also, the curve-fitting algorithm created problems in some short creep tests. We have considered previously the advantages and drawbacks of testing cadaveric tissues,[29] and the use of the present apparatus.[22]

Relationship to other studies. Comparable deformations have been reported previously in cadaveric spines, although not simultaneously in discs and vertebrae. Lower thoracic vertebral bodies from young men deform by 0.15 - 0.20 mm per kN of applied load, and by 2 - 3 mm before collapsing (calculated from[30]). Equivalent values for severely osteoporotic old vertebral bodies are 0.7 mm deformation per kN, and 1.5 mm before collapse.[7] Vertebral deformations in Figure 4 and Table 1 lie between these extremes. Few previous studies have separated the deformations of intervertebral discs from those of adjacent bone, but those that did so found the discs to be surprisingly stiff. A high-resolution MRI study on cadaveric motion segments reported 0.4 mm vertical disc deformation in response to a compressive force of 1 kN applied for 26 min.[19] This compares with a total (elastic+0.5 hr creep) disc height loss of 0.2 mm in the present study (Figure 4). Similarly, a stereo photographic technique showed that elastic disc height loss in response to 2.5 kN compression averaged 0.67 mm anteriorly and 0.83 posteriorly[18] which is equivalent to 0.3 mm at a compressive force of 1 kN. The slightly lower compressive deformability of the disc in the present

experiment (Figure 4) may be attributable to stress-shielding by the neural arch, because this structure was removed in the previously-mentioned experiments.

The phenomenon of creep deformation in ageing human vertebrae has been described recently by our laboratory[10, 11] and was anticipated by Keller et al.[28] who showed that vertebral BMD influenced the *time dependent* properties of a motion segment. It has also been reported in young porcine motion segments,[31] although true bone creep was difficult to distinguish from creep in the hyaline cartilage endplate. This latter study suggested that disc creep becomes *relatively* more important as a loading test continues, which is consistent with the major influence of IDP found in the present study: as creep progresses, nucleus water content[23] and IDP[32] both fall, allowing the disc to bulge radially.[18, 33] Bulging increases the tendency for the annulus to deform viscoelastically by mechanisms such as interfibrillar sliding[34] that do not depend on fluid flow.[35]

Values of E1, E2 and η in Tables 2 and 3 agree with those reported previously by researchers using the same model[27, 28, 36] provided that allowance is made for the influence of test duration (Figure 5). These previous studies also showed similar trends with increasing age, although too few specimens were tested to resolve the competing influences of spinal level, disc dimensions, and disc degeneration. The model can be used to represent disc behaviour only, but the excellent agreement between experimental and predicted deformations in the current study show that it is well suited to analyse height loss by an entire motion segment, including the neural arch (Figure 2).

Explanation of results Disc tissues are virtually incompressible when loaded rapidly, so compressive elastic deformation of a motion segment occurs by the endplates bulging into the vertebral bodies[8] and by the disc bulging radially outwards.[18, 33] Trabecular bone within the vertebral body is compacted as trabeculae buckle[37] and the vertebral body cortex probably bulges radially.[38] A high IDP prestresses both annulus and endplate, and prevents either from bulging greatly when loading is increased. E1 and E2 represent the modulus (stress/strain) for the drained and hydrated motion segment respectively, so it is not surprising that they depend on disc area (which determines applied stress) because most biological materials become stiffer when compressed more severely. When loading is sustained, elastic deformations are followed by creep, as water is expelled from the disc.[23] Disc creep recovers when loading is removed, both *in vivo* and *in vitro*, because expelled water is sucked back in again.[39, 40] In vertebral bone, various time-dependent processes occur which are still poorly understood,[15] but which include micro-crack propagation.[41] Bone creep does not recover quickly,[11, 15] and may not recover completely, at least in cadaveric experiments, because plastic deformation could be involved. In the model, time dependent processes are indicated by the viscosity η which also depends primarily on IDP. High

IDP reflects a high proteoglycan content in the nucleus, and these hydrophilic molecules resist water expulsion under load, slowing the creep process.

Deformations of discs and vertebrae increase in old age (Table 3) primarily because of falling IDP.[24] As the proteoglycan and water content of the nucleus decrease, IDP falls,[22, 32] annulus bulging increases[26] and stress concentrations arise within the annulus[24] severely compressing the vertebral cortex. The annulus and endplate are no longer prestressed by the nucleus, and so can deform more when external loading increases. Proteoglycan depletion in the nucleus reduces its ability to prevent water loss under load, so creep rate increases. However, the extent of creep may decrease because old discs have less water to lose[42, 43] and so reach equilibrium faster.[44] The high elastic deformability of old vertebral bodies[7] appears to be a consequence of reduced bone *mass* allowing increased buckling of trabeculae and cortex. Compressive deformations of ageing motion segments rarely increase beyond 3 mm because adjacent neural arches become load-bearing in erect postures[4] and oppose further height loss. Load-bearing increases substantially after just 1 mm height loss[45] so that, in old spines with severely degenerated discs, the neural arch typically resists 63% of an applied axial compressive force, with the anterior and posterior halves of the vertebral body resisting just 10% and 26% respectively.[46] Some of these age-related mechanisms were proposed by Kazarian more than 30 years ago,[44] although detailed experimental evidence was lacking.

The foregoing discussion suggests that the changing compressibility of ageing spines is primarily due to *structural* changes including reduced nucleus volume and IDP, reduced anterior bone mass, and impaction of neural arches. The influence of altered materials properties of old anulus and bone appear to be slight; in fact, ageing annulus[47, 48] and bone[49] tissues show little tendency to soften and weaken, and increased collagen cross-linking actually stiffens old cartilage[50] and bone.[51]

Some other influences on motion segment deformations are apparent from Tables 2 and 3. E2 and η are greater in females (Table 2) because female discs tend to have a smaller cross-sectional area, and so were subjected to higher compressive stress in the present experiments. Viscosity η probably increases with stress because the high tissue deformation at high stress reduces pore size, and hence the rate of fluid expulsion.[52] Vertebral bodies deform more anteriorly than posteriorly (Table 1) because elderly vertebrae suffer most bone loss from their anterior regions,[53, 54] probably as a result of being stress-shielded by the neural arch following disc collapse.[46] Discs deform more posteriorly than anteriorly because compressive stresses tend to be concentrated there with increasing age and degeneration.[24, 55] The fact that total height loss by the three structures (two vertebrae and the disc) is greater anteriorly than posteriorly (last line in Table 1) suggests unequal deformations in the apparatus and at the bone-plaster junction.

Clinical implications. Lumbar spinal stenosis affects approximately 13% of patients referred to spine specialists in the USA,[2] and it becomes increasingly common after middle age. The results of the present study indicate that, when a physically active elderly person stands up after a period of rest, each thoracolumbar motion segment will lose an average 0.87 mm in height, followed by a further 1.37 mm during the following two hours (Table 4). This total height loss (2.24 mm) is approximately 10% of the height of a typical lumbar intervertebral foramen.[56] However, nerve-root compression is typically found in intervertebral foramina that are narrowed by only 1.4 - 4.5 mm compared to L1-L5 foramina with normal nerve roots.[56] Of course, patients with nerve-root compression may not *be* typical, and the maximum height loss recorded in the present experiment after 2 hr (4.5 mm) might well cause problems. Also, disc height loss is accompanied by a proportional increase in radial bulging[18, 26] so both diameters of the intervertebral foramen tend to be reduced at the same time. These quantitative comparisons are approximate only, for several reasons. Firstly, it would have been more accurate to compare foramen height with height loss by a *single* disc and vertebra, rather than by a motion segment, but this information was not available for most specimens. Also, small *horizontal* movements of adjacent vertebrae could influence the height of the foramen, and spinal loading (and deformations) would all be reduced in elderly people who are no longer physically active. Nevertheless, the above comparisons suggest that nerve root entrapment syndromes can occur as a result of transient compressive deformations of the spine, even in the absence of permanent structural changes such as disc herniation, osteophytosis or spondylolysthesis. Any such "functional stenosis" would be influenced by posture, which can have a profound influence on disc height loss and bulging,[57, 58] and on resulting symptoms.[2]

A second clinical consequence of disc creep is that the resulting fluid exchange can aid in disc nutrition.[23, 59] Results of the present experiment suggest that this boost to metabolite transport diminishes in old age, because the discs have less water to lose, and because creep is limited by the neural arch. This protective action of the neural arch can have clinical consequences in it own right, because high load-bearing by the apophyseal joints, above a certain threshold, is closely associated with osteoarthritic changes.[5]

Unanswered questions and future research. The mechanisms of vertebral creep are currently under investigation in a number of laboratories, including our own. It may well depend on bone mineral density.

References

1. Venner RM, Crock HV. Clinical studies of isolated disc resorption in the lumbar spine. J Bone Joint Surg [Br] 1981;4:491-4.

2. Watters WC, 3rd, Baisden J, Gilbert TJ, et al. Degenerative lumbar spinal stenosis: an evidence-based clinical guideline for the diagnosis and treatment of degenerative lumbar spinal stenosis. Spine J 2008;8(2):305-10.
3. Malmivaara A, Slatis P, Heliovaara M, et al. Surgical or nonoperative treatment for lumbar spinal stenosis? A randomized controlled trial. Spine 2007;32(1):1-8.
4. Pollintine P, Przybyla AS, Dolan P, Adams MA. Neural arch load-bearing in old and degenerated spines. J Biomech 2004;37(2):197-204.
5. Brown KR, Pollintine P, Adams MA. Biomechanical implications of degenerative joint disease in the apophyseal joints of human thoracic and lumbar vertebrae. Am J Phys Anthropol 2008;136(3):318-26.
6. Butler D, Trafimow JH, Andersson GB, McNeill TW, Huckman MS. Discs degenerate before facets. Spine 1990;15(2):111-3.
7. Molloy S, Mathis JM, Belkoff SM. The effect of vertebral body percentage fill on mechanical behavior during percutaneous vertebroplasty. Spine 2003;28(14):1549-54.
8. Brinckmann P, Frobin W, Hierholzer E, Horst M. Deformation of the vertebral end-plate under axial loading of the spine. Spine 1983;8(8):851-6.
9. Green TP, Allvey JC, Adams MA. Spondylolysis. Bending of the inferior articular processes of lumbar vertebrae during simulated spinal movements. Spine 1994;19(23):2683-91.
10. Pollintine P, Offa-Jones B, Dolan P, Adams MA. Bone creep and vertebral deformity. In: European Society of Biomechanics; 2006; Munich; 2006.
11. Pollintine P, Luo J, Offa-Jones B, Dolan P, Adams MA. Bone creep can cause progressive vertebral deformity. Spine (submitted for publication) 2008.
12. Sato K, Kikuchi S, Yonezawa T. In vivo intradiscal pressure measurement in healthy individuals and in patients with ongoing back problems. Spine 1999;24(23):2468-74.
13. Dolan P, Earley M, Adams MA. Bending and compressive stresses acting on the lumbar spine during lifting activities. J Biomech 1994;27(10):1237-48.
14. Bowman SM, Keaveny TM, Gibson LJ, Hayes WC, McMahon TA. Compressive creep behavior of bovine trabecular bone. J Biomech 1994;27(3):301-10.
15. Yamamoto E, Paul Crawford R, Chan DD, Keaveny TM. Development of residual strains in human vertebral trabecular bone after prolonged static and cyclic loading at low load levels. J Biomech 2006;39(10):1812-8.
16. Adams MA, Luo J, Pollintine P, Dolan P. Creep deformity of human vertebrae. In: Britspine; 2008; Belfast (accepted); 2008.
17. Heuer F, Schmidt H, Wilke HJ. The relation between intervertebral disc bulging and annular fiber associated strains for simple and complex loading. J Biomech 2008;41(5):1086-94.

18. Stokes IA. Bulging of lumbar intervertebral discs: non-contacting measurements of anatomical specimens. J Spinal Disord 1988;1(3):189-93.
19. O'Connell GD, Johannessen W, Vresilovic EJ, Elliott DM. Human internal disc strains in axial compression measured noninvasively using magnetic resonance imaging. Spine 2007;32(25):2860-8.
20. Adams MA, Dolan P, Hutton WC. The stages of disc degeneration as revealed by discograms. J Bone Joint Surg [Br] 1986;68(1):36-41.
21. Adams MA, Bogduk N, Burton K, Dolan P. The Biomechanics of Back Pain. (2nd Edition). Churchill Livingstone, Edinburgh; 2006.
22. Zhao F, Pollintine P, Hole BD, Dolan P, Adams MA. Discogenic origins of spinal instability. Spine 2005;30(23):2621-30.
23. McMillan DW, Garbutt G, Adams MA. Effect of sustained loading on the water content of intervertebral discs: implications for disc metabolism. Ann Rheum Dis 1996;55(12):880-7.
24. Adams MA, McNally DS, Dolan P. 'Stress' distributions inside intervertebral discs. The effects of age and degeneration. J Bone Joint Surg Br 1996;78(6):965-72.
25. Chu JY, Skrzypiec D, Pollintine P, Adams MA. Can compressive stress be measured experimentally within the annulus fibrosus of degenerated intervertebral discs? Proc Inst Mech Eng [H] 2008;222(2):161-70.
26. Brinckmann P, Grootenboer H. Change of disc height, radial disc bulge, and intradiscal pressure from discectomy. An in vitro investigation on human lumbar discs. Spine 1991;16(6):641-6.
27. Burns ML, Kaleps I, Kazarian LE. Analysis of compressive creep behavior of the vertebral unit subjected to a uniform axial loading using exact parametric solution equations of Kelvin-solid models--Part I. Human intervertebral joints. J Biomech 1984;17(2):113-30.
28. Keller TS, Spengler DM, Hansson TH. Mechanical behavior of the human lumbar spine. I. Creep analysis during static compressive loading. J Orthop Res 1987;5(4):467-78.
29. Adams MA. Mechanical testing of the spine. An appraisal of methodology, results, and conclusions. Spine 1995;20(19):2151-6.
30. Kazarian L, Graves GA. Compressive strength characteristics of the human vertebral column. Spine 1977;2(1):1-14.
31. van der Veen AJ, Mullender MG, Kingma I, van JH, Smit TH. Contribution of verftebral bodies, endplates, and intervertebral discs to the compression creep of spinal motion segments. J Biomech 2008;41(6):1260-8.
32. Adams MA, McMillan DW, Green TP, Dolan P. Sustained loading generates stress concentrations in lumbar intervertebral discs. Spine 1996;21(4):434-8.

33. Brinckmann P, Horst M. The influence of vertebral body fracture, intradiscal injection, and partial discectomy on the radial bulge and height of human lumbar discs. Spine 1985;10(2):138-45.
34. Duncan NA. Cell deformation and micromechanical environment in the intervertebral disc. J Bone Joint Surg Am 2006;88 Suppl 2:47-51.
35. Koeller W, Funke F, Hartmann F. Biomechanical behavior of human intervertebral discs subjected to long lasting axial loading. Biorheology 1984;21(5):675-86.
36. Li S, Patwardhan AG, Amirouche FM, Havey R, Meade KP. Limitations of the standard linear solid model of intervertebral discs subject to prolonged loading and low-frequency vibration in axial compression. J Biomech 1995;28(7):779-90.
37. Nicholson PH, Cheng XG, Lowet G, et al. Structural and material mechanical properties of human vertebral cancellous bone. Med Eng Phys 1997;19(8):729-37.
38. Kopperdahl DL, Roberts AD, Keaveny TM. Localized damage in vertebral bone is most detrimental in regions of high strain energy density. J Biomech Eng 1999;121(6):622-8.
39. Botsford DJ, Esses SI, Ogilvie-Harris DJ. In vivo diurnal variation in intervertebral disc volume and morphology. Spine 1994;19(8):935-40.
40. van der Veen AJ, van Dieen JH, Nadort A, Stam B, Smit TH. Intervertebral disc recovery after dynamic or static loading in vitro: Is there a role for the endplate? J Biomech 2007;40(10):2230-5.
41. Zioupos P, Hansen U, Currey JD. Microcracking damage and the fracture process in relation to strain rate in human cortical bone tensile failure. J Biomech 2008;41(14):2932-9.
42. Antoniou J, Steffen T, Nelson F, et al. The human lumbar intervertebral disc: evidence for changes in the biosynthesis and denaturation of the extracellular matrix with growth, maturation, ageing, and degeneration. J Clin Invest 1996;98(4):996-1003.
43. Adams MA, Hutton WC. The effect of posture on the fluid content of lumbar intervertebral discs. Spine 1983;8(6):665-71.
44. Kazarian LE. Creep characteristics of the human spinal column. Orthop Clin North Am 1975;6(1):3-18.
45. Dunlop RB, Adams MA, Hutton WC. Disc space narrowing and the lumbar facet joints. J Bone Joint Surg [Br] 1984;66(5):706-10.
46. Adams MA, Pollintine P, Tobias JH, Wakley GK, Dolan P. Intervertebral disc degeneration can predispose to anterior vertebral fractures in the thoracolumbar spine. J Bone Miner Res 2006;21(9):1409-16.
47. Acaroglu ER, Iatridis JC, Setton LA, Foster RJ, Mow VC, Weidenbaum M. Degeneration and aging affect the tensile behavior of human lumbar anulus fibrosus. Spine 1995;20(24):2690-701.

48. Skrzypiec D, Tarala M, Pollintine P, Dolan P, Adams MA. When are intervertebral discs stronger than their adjacent vertebrae? Spine 2007;32(22):2455-61.
49. Rho JY, Zioupos P, Currey JD, Pharr GM. Microstructural elasticity and regional heterogeneity in human femoral bone of various ages examined by nano-indentation. J Biomech 2002;35(2):189-98.
50. Verzijl N, DeGroot J, Ben ZC, et al. Crosslinking by advanced glycation end products increases the stiffness of the collagen network in human articular cartilage: a possible mechanism through which age is a risk factor for osteoarthritis. Arthritis Rheum 2002;46(1):114-23.
51. Banse X, Sims TJ, Bailey AJ. Mechanical properties of adult vertebral cancellous bone: correlation with collagen intermolecular cross-links. J Bone Miner Res 2002;17(9):1621-8.
52. Heneghan P, Riches PE. Determination of the strain-dependent hydraulic permeability of the compressed bovine nucleus pulposus. J Biomech 2008;41(4):903-6.
53. Antonacci MD, Hanson DS, Leblanc A, Heggeness MH. Regional variation in vertebral bone density and trabecular architecture are influenced by osteoarthritic change and osteoporosis. Spine 1997;22(20):2393-401; discussion 401-2.
54. Zhao FD, Pollintine P, Hole BD, Adams MA, Dolan P. Vertebral fractures usually affect the cranial endplate because it is thinner and supported by less-dense trabecular bone. Bone 2008.
55. Adams MA, May S, Freeman BJ, Morrison HP, Dolan P. Effects of backward bending on lumbar intervertebral discs. Relevance to physical therapy treatments for low back pain. Spine 2000;25(4):431-7; discussion 8.
56. Hasegawa T, An HS, Haughton VM, Nowicki BH. Lumbar foraminal stenosis: critical heights of the intervertebral discs and foramina. A cryomicrotome study in cadavera. J Bone Joint Surg Am 1995;77(1):32-8.
57. Panjabi MM, Takata K, Goel VK. Kinematics of lumbar intervertebral foramen. Spine 1983;8(4):348-57.
58. Fujiwara A, An HS, Lim TH, Haughton VM. Morphologic changes in the lumbar intervertebral foramen due to flexion-extension, lateral bending, and axial rotation: an in vitro anatomic and biomechanical study. Spine 2001;26(8):876-82.
59. Ferguson SJ, Ito K, Nolte LP. Fluid flow and convective transport of solutes within the intervertebral disc. J Biomech 2004;37(2):213-21.

Figure Captions

Figure 1 Apparatus used to compress cadaveric motion segments. The low-friction rollers ensured only compressive loading was applied. In 17 experiments, six reflective markers secured to each

vertebral body were tracked by an optical system (MacReflex) in order to measure vertical deformations of the disc and each vertebral body in the sagittal plane.

Figure 2 The three-parameter model consists of a spring E2, which resists elastic deformation, a dashpot or syringe (η) which resists fluid flow, and a second spring E1 which resists deformation of the "drained" structure. E1, E2 and η are calculated from the height and area of the intervertebral disc, but when the model is applied to a whole motion segment, E1 includes resistance from the neural arch, as suggested by the Figure. Note the radiographically dense bone in the neural arch, indicative of the high load-bearing often found in elderly spines.

Figure 3 Typical data for a 0.5 hr test, showing elastic and creep strains of the two vertebral bodies and the intervening disc, as measured by the MacReflex. Strains were averaged for the anterior, middle and posterior region of each structure. In this specimen (Male, 82 yr, T11-T12) elastic strain was approximately 50% greater in the disc compared to vertebral bodies, and creep strain was 300-400% greater. 10,000 microstrains = deformation of 1%.

Figure 4 Average height loss by the upper vertebra, disc and lower vertebra during 30 min tests (n=17, error bars = SEM). Initial elastic deformations were greater in the vertebral bodies compared to the disc, but creep was similar in all three structures.

Figure 5 Model parameters E1, E2 and η varied systematically with the duration of loading. Data for 52 specimens at 0.5 hr, 102 for 1 hr, and 84 for 2 hr. Error bars indicate the STD.

Figure 6 The elastic modulus (E2) of 84 motion segments subjected to 2 hr tests decreased with age. Regression data refer to 73 of the specimens that were aged >50 yr. E2 tended to *increase* up to the age of 40.

Figure 7 Viscosity (η) increased with intradiscal pressure (IDP) in the 2 hr tests. IDP was measured for 60 of the 84 specimens tested for 2 hr.

Figure 8 Total compressive deformation of thoracolumbar motion segments increased above 50 yr of age (r^2=0.06, p = 0.023). Regression data for 90 of the 102 specimens compressed by 1 kN for 1 hr. Deformation *decreased* in 12 specimens aged 19-47 yr (p=0.07).

Table 1 Compressive deformations of discs and vertebral bodies (VB) in 17 motion segments tested for 0.5 hr. Values indicate the mean (STD). Elastic and creep deformations are presented separately for the posterior (Post.), middle, and anterior (Ant.) regions of the disc and vertebral bodies (VB).

		Compressive deformation (height loss) in mm					
		Elastic			Creep		
		Post.	Middle	Ant.	Post.	Middle	Ant.
Upper VB	mean	**0.16**	**0.20**	**0.28**	**0.03**	**0.14**	**0.16**
	std	0.21	0.26	0.41	0.06	0.26	0.26
Disc	mean	**0.11**	**0.11**	**0.02**	**0.13**	**0.13**	**0.08**
	std	0.12	0.18	0.11	0.09	0.13	0.10
Lower VB	mean	**0.08**	**0.16**	**0.35**	**0.03**	**0.09**	**0.21**
	std	0.14	0.44	0.80	0.11	0.33	0.43
Total		0.35	0.47	0.66	0.19	0.36	0.45

Table 2: Average values of parameters from 2 hr tests for various groups of specimens. These values varied between the 0.5, 1 and 2 hr tests as shown in **Figure 5**.

	n	**E1 (MPa)**	**E2(MPa)**	**η1 (GPa*s)**	**E2/E1**
All	84	4.80	8.56	36.7	2.05
Male	39	4.84	6.99	30.7	1.60
Female	45	4.77	9.92	41.9	2.44
Age ≤ 75 year	45	4.64	9.62	41.2	2.36
Age > 75 year	39	4.99	7.33	31.7	1.69
Degeneration 1-2	37	4.57	10.43	45.1	2.64
Degeneration 3-4	47	4.98	7.08	30.2	1.59
Thoracic	27	4.92	10.99	45.9	2.81
Lumbar	57	4.75	7.40	32.5	1.69

Table 3 Univariate linear regression analyses showed major influences on model parameters from the 2 hr tests. Bold text indicates significant relationships. Spinal levels are coded from 1 (T7-8) to 10 (L4-5). a1 and a2 are coefficients from the equation: y = a1*x + a2.

	Parameter	n	r^2	p	a1	a2
Age (yrs)	E1 (MPa)	84	0.01	0.417	-0.0105	5.51
	E2 (MPa)	84	0.09	**0.006**	-0.0717	13.4
	η (GPa*s)	84	0.09	**0.006**	-0.3119	57.9
Disc degen. grade	E1 (MPa)	84	0.00	0.917	-0.0333	4.88
	E2 (MPa)	84	0.12	**0.001**	-2.052	13.9
	η (GPa*s)	84	0.13	**<0.001**	-9.413	61.3
Spinal level	E1 (MPa)	84	0.00	0.639	0.0474	4.50
	E2 (MPa)	84	0.16	**<0.001**	-0.7512	13.2
	η (GPa*s)	84	0.11	**0.002**	-2.6686	53.4
Disc area (mm^2)	E1 (MPa)	84	0.02	0.175	-0.0008	5.91
	E2 (MPa)	84	0.39	**<0.001**	-0.0066	18.0
	η (GPa*s)	84	0.32	**<0.001**	-0.0261	74.3
Applied stress (MPa)	E1 (MPa)	84	0.21	**<0.001**	3.360	2.01
	E2 (MPa)	84	0.29	**<0.001**	7.994	1.92
	η (GPa*s)	84	0.15	**<0.001**	25.39	15.7
IDP (MPa)	E1 (MPa)	60	0.02	0.333	-0.3795	5.01
	E2 (MPa)	60	0.32	**<0.001**	4.268	3.73
	η (GPa*s)	60	0.33	**<0.001**	17.40	17.1

Table 4: Summary of motion segment elastic and creep compressive deformations. Mean values are shown (STD).

				Deformation (mm)		
Duration (hrs)	Age (yrs)	Applied Stress (MPa)	n	Elastic	Creep	Total
2	68 (18)	0.83 (0.29)	84	**0.87** (0.44)	**1.37** (0.46)	**2.24** (0.60)
1	68 (17)	0.85 (0.28)	100	**0.84** (0.43)	**0.71** (0.29)	**1.55** (0.72)
0.5	65 (20)	0.81 (0.29)	52	**0.62** (0.49)	**0.54** (0.38)	**1.16** (0.86)

Figure 1

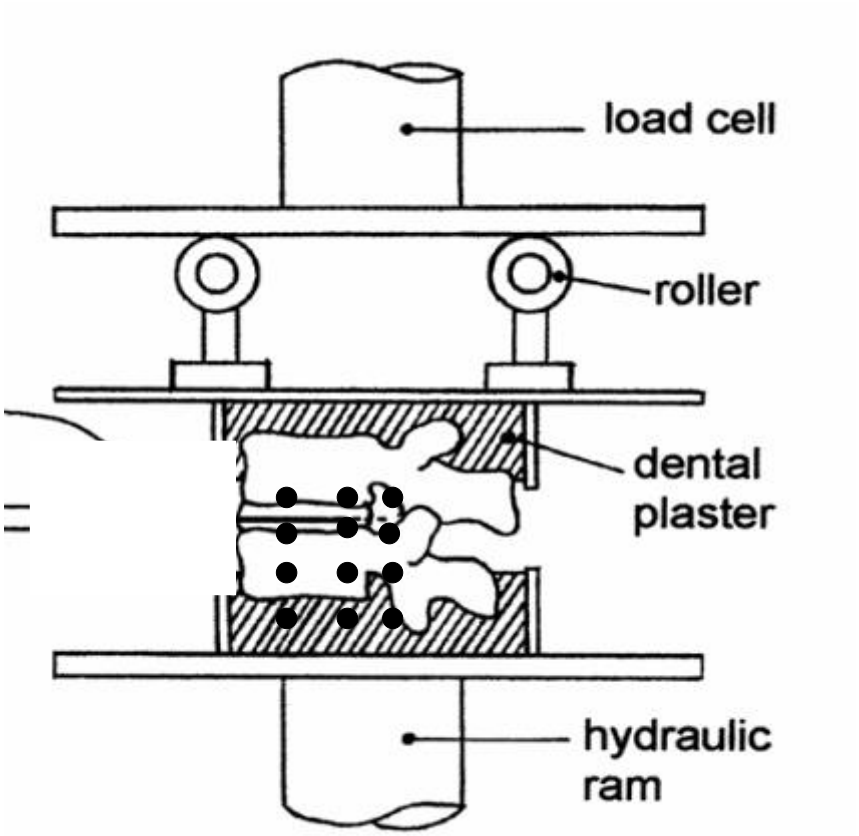

Figure 2

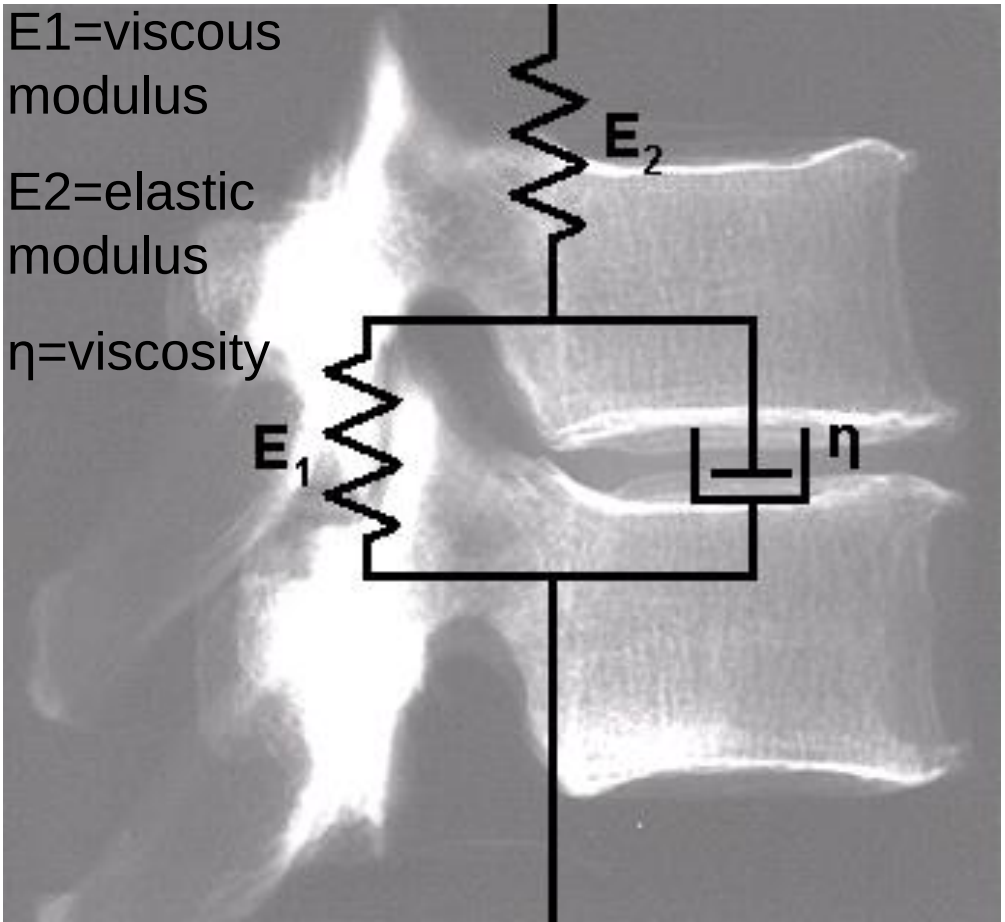

Figure 3

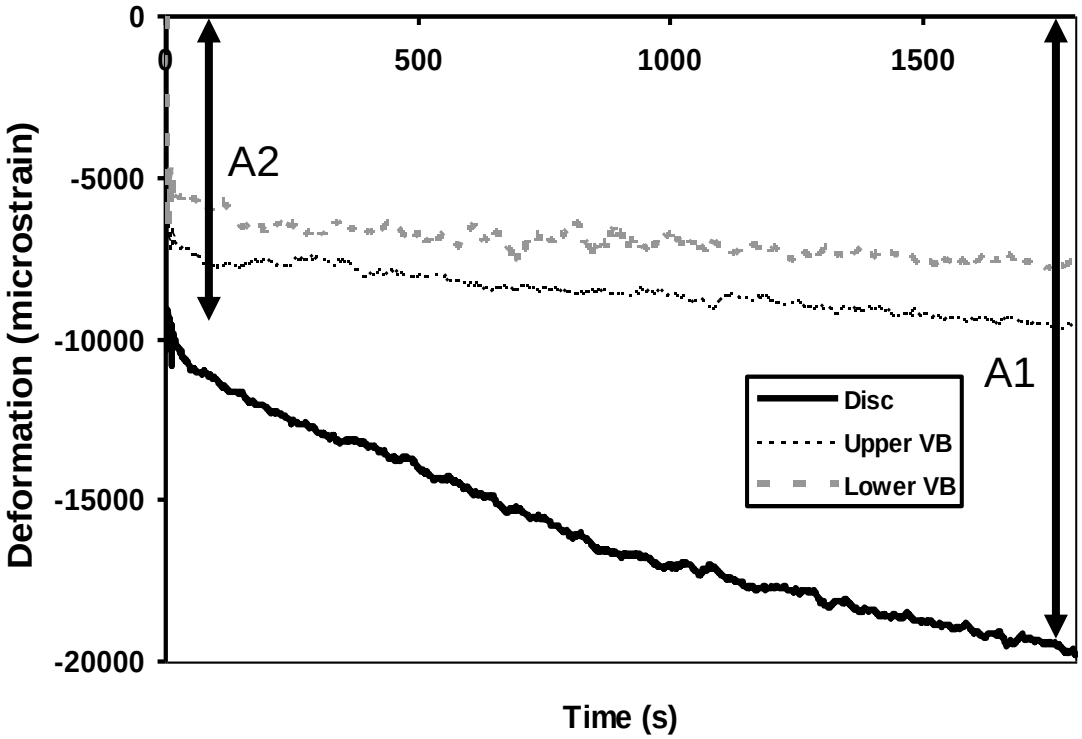

Figure 4

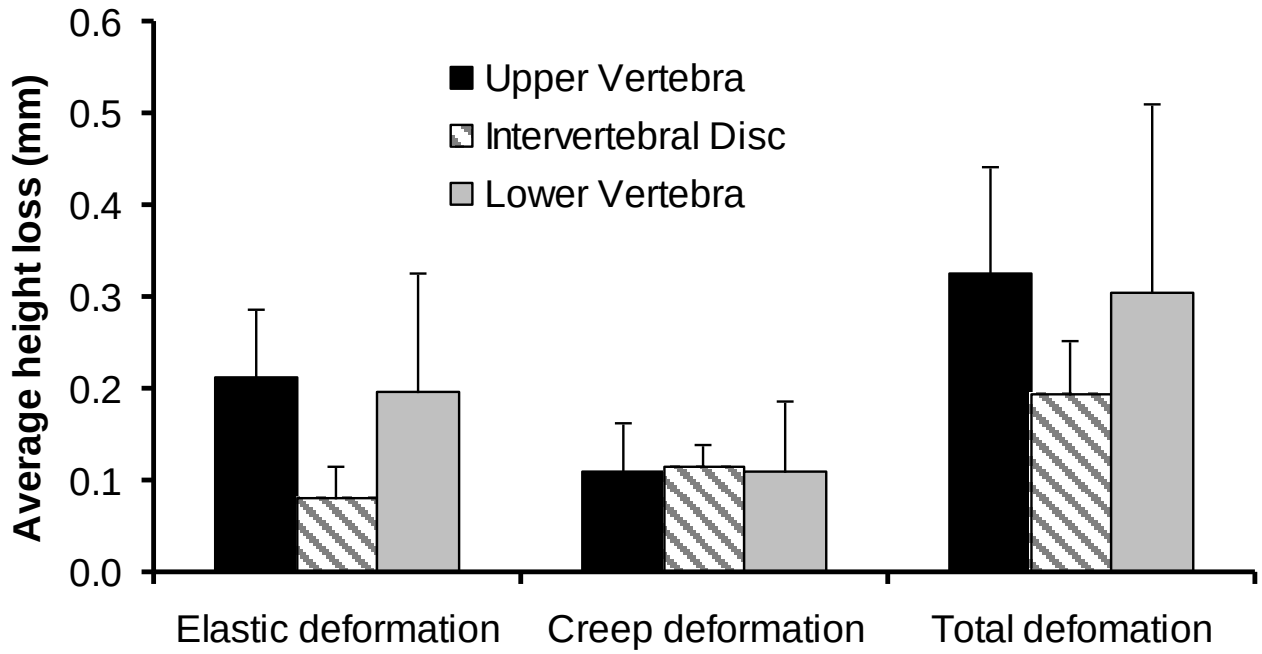

Figure 5

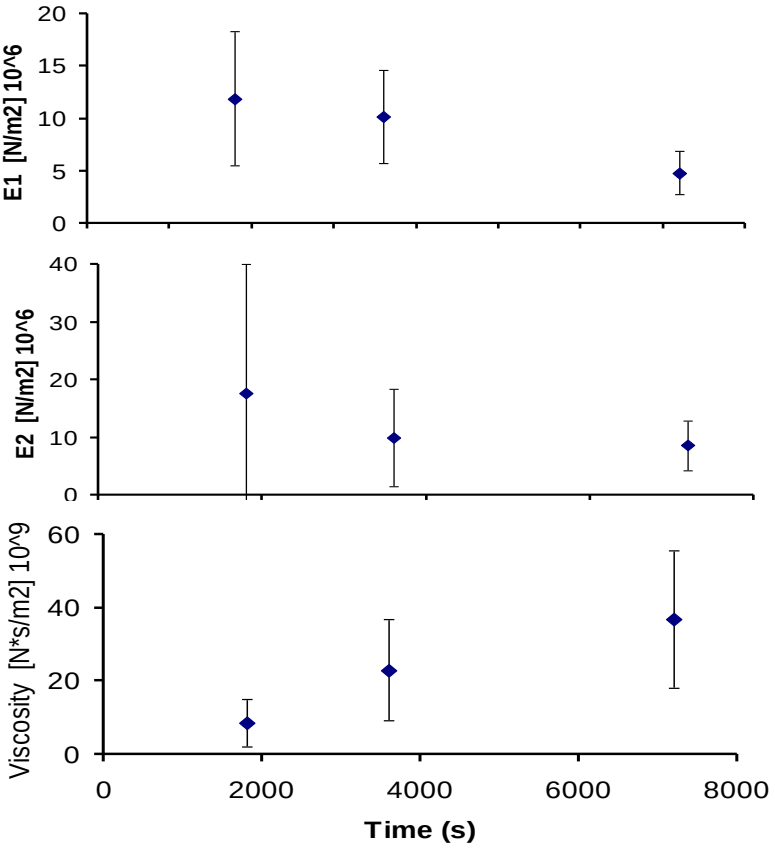

Figure 6

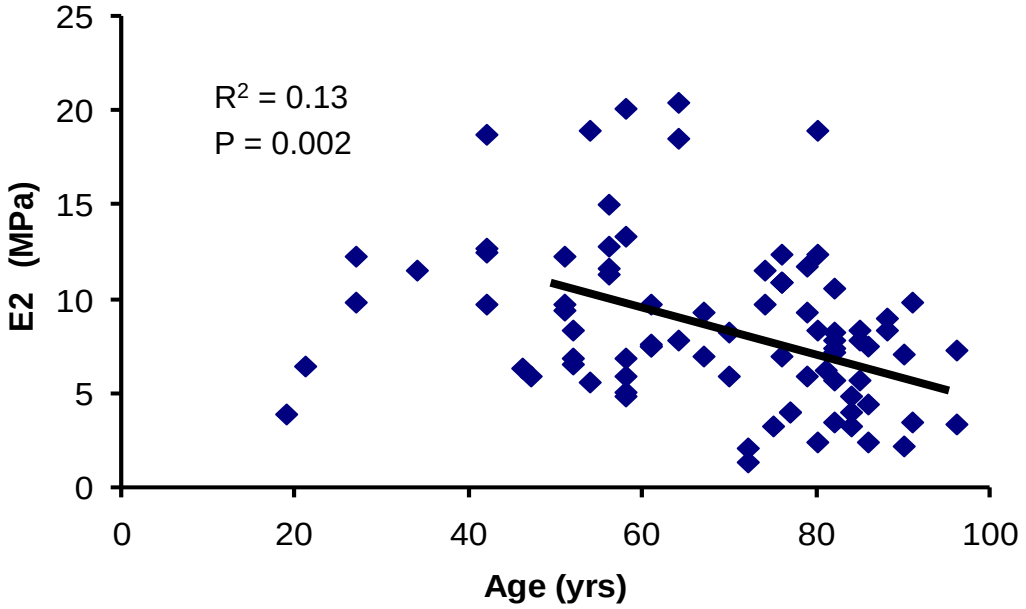

Figure 7

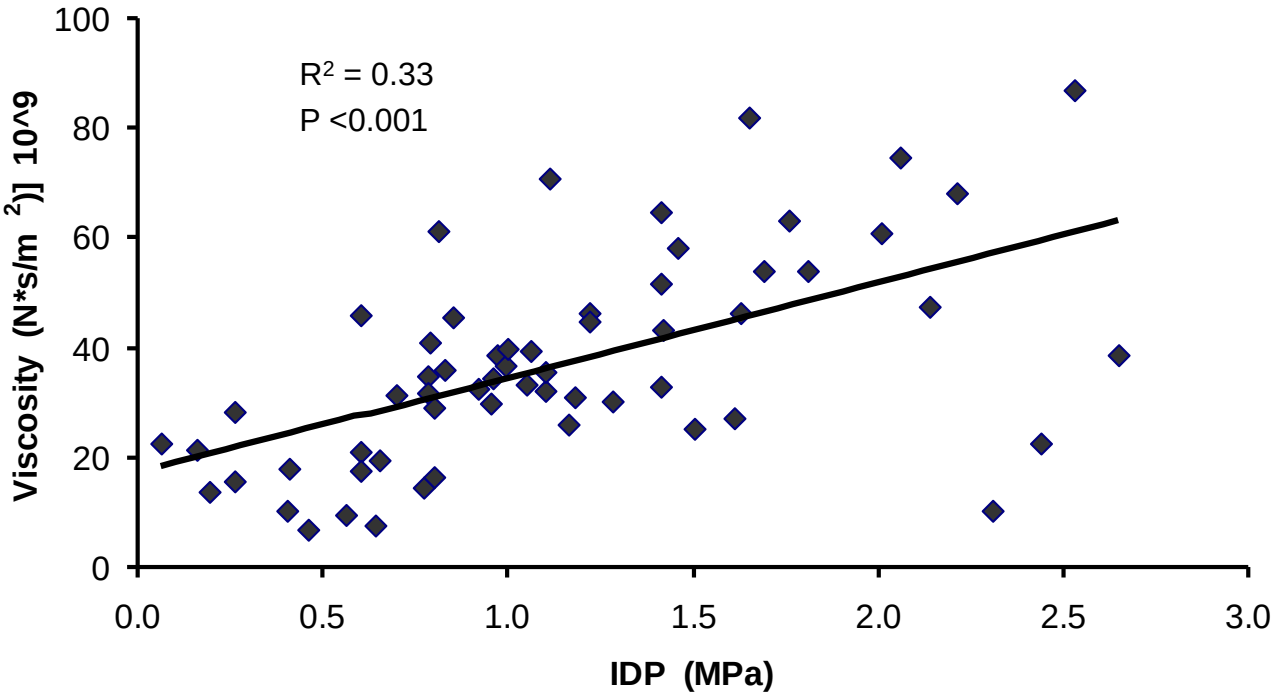

Figure 8